Challenging the cholinergic system : ageing, cognition & inflammation
Alvarez-Jiménez, R.

Citation
Alvarez-Jiménez, R. (2017, June 1). *Challenging the cholinergic system : ageing, cognition & inflammation*. Retrieved from https://hdl.handle.net/1887/49260

Cover Page

Universiteit Leiden

Author: Alvarez-Jiménez, Ricardo
Title: Challenging the cholinergic system : ageing, cognition & inflammation
Issue Date: 2017-06-01

EEG MACHINE LEARNING FOR ACCURATE DETECTION OF CHOLINERGIC INTERVENTION AND ALZHEIMER'S DISEASE

S. Simpraga, R. Alvarez-Jimenez,
H. D. Mansvelder, J. M. A. van Gerven,
G. J. Groeneveld, S.-S. Poil,
K. Linkenkaer-Hansen

ABSTRACT

Monitoring effects of disease or therapeutic intervention on brain function is increasingly important for clinical trials, albeit hampered by inter-individual variability and subtle effects. Here, we apply complementary biomarker algorithms to electroencephalography (EEG) recordings to capture the brain's multi-faceted signature of disease or pharmacological intervention and use machine learning to improve classification performance. Using data from healthy subjects receiving scopolamine we developed an index of the muscarinic acetylcholine receptor antagonist (mAChR) consisting of 14 EEG biomarkers. This mAChR index yielded higher classification performance than any individual EEG biomarker with cross-validated accuracy, sensitivity, specificity and precision ranging from 88–92%. The mAChR index also discriminated healthy elderly from patients with Alzheimer's disease (AD); however, an index optimized for AD pathophysiology provided a better classification. We conclude that integrating multiple EEG biomarkers can enhance the accuracy of identifying disease or drug interventions, which is essential for clinical trials.

INTRODUCTION

An increasing number of drug candidates are being tested for their ability to modify disease or alleviate symptoms of brain disorders (Van der Schyf and Geldenhuys, 2011); however, to test these new pharmacological interventions and improve monitoring of the therapeutic response, informative and robust endpoints are urgently needed (Frank and Hargreaves, 2003; Golde, 2016; Oertel and Schulz, 2016). Clinical trials in central nervous system (CNS) drug development focus on behavioral and cognitive performance outcome measures of drug efficacy; however, quantitative electroencephalography (EEG) is gaining recognition in the field as a source of surrogate endpoints in early-phase studies (van Straaten *et al*, 2014). EEG offers insight into the mode of action of the pharmacological intervention, because of the high temporal resolution of electrophysiological measures (Leiser *et al*, 2011; Lopes da Silva, 2013). Still, it remains an important challenge to advance EEG biomarker analysis for enhanced prediction of therapeutic effects in clinical trials.

Scopolamine is the most extensively used pharmacological model of cognitive impairment (Klinkenberg and Blokland, 2010). As a selective competitive muscarinic receptor (mAChR) antagonist, it induces temporary deficits in cognitive functions that depend on the cholinergic system (Ebert *et al*, 1998). Scopolamine has a high affinity for all five muscarinic receptor subtypes (M_1–M_5) and a negligible affinity for histaminergic and dopaminergic receptors (Ali-Melkkilä *et al*, 1993). Muscarinic receptors are widely present in brain areas involved in attention and memory, and intravenous administration of scopolamine indeed causes impairments to these brain functions (Broks *et al*, 1988; Liem-Moolenaar *et al*, 2011). The scopolamine challenge test has been used in drug development to demonstrate the pharmacological activity of putatively cognition-enhancing compounds by reversal of scopolamine-induced cognitive deficits in healthy volunteers (Cho *et al*, 2011; Jones *et al*, 1991; Liem-Moolenaar *et al*, 2010a, 2010b; Preda *et al*, 1993; Prohovnik *et al*, 1997; Siegfried, 1993; Snyder *et al*, 2005).

EEG biomarkers have the potential to objectively determine whether reversal of scopolamine effects by a cholinergic compound is successful. In humans, scopolamine administration increases the power of delta and

theta activity, while alpha- and beta-frequency activity is reduced (Alvarez-Jimenez *et al*, 2016; Ebert *et al*, 1998; Liem-Moolenaar *et al*, 2011). It has been hypothesized that deficits of cholinergic signaling contribute to the EEG slowing in Alzheimer's disease (Agnoli *et al*, 1983; Blennow *et al*, 2006), which is also supported by the reversal of EEG slowing by cholinergic drugs (Citron, 2010; Jeong, 2004). Unfortunately, current biomarkers lack the desired accuracy for monitoring disease status or therapeutic response, because of large inter-individual variability compared to the often subtle drug-related changes. Most commonly, the functional state of the brain is assessed merely using one type of biomarker (Babiloni *et al*, 2004; Osipova *et al*, 2005; Sankari *et al*, 2012; Stam *et al*, 2003); however, pathophysiology is often expressed as changes to multiple properties of neuronal oscillations. Consequently, different biomarker algorithms may quantify distinct aspects of the brain's functional state. Combining these may increase accuracy of disease diagnosis and assessment of drug interventions (Dauwels *et al*, 2010b; Khodayari-Rostamabad *et al*, 2010; Lehmann *et al*, 2007; Montez *et al*, 2009; Poil *et al*, 2013). Here, we use machine learning to show that the complementary information of different EEG biomarkers can indeed be combined into an accurate index for better decision-making in clinical trials.

METHODS
SUBJECTS

Data were obtained from four separate trials conducted at the Centre of Human Drug Research (Leiden, the Netherlands) and approved by a medical ethics committee. All subjects signed a written informed consent prior to participation in the study and were medically screened.

Trial 1 and 2 evaluated the effect of investigational glycinergic compounds during a cognitive impairment scopolamine challenge test. A detailed description of the neurophysiologic tests has been reported previously (Liem-Moolenaar *et al*, 2010a, 2010b). In the two trials, a total of 83 male healthy subjects aged 18–55 years were recruited. Scopolamine (0.5 mg) or placebo was administered as a 15-minute intravenous infusion. Only the data where subjects received placebo or scopolamine (alone) was used in the

analysis. Study periods were separated by a washout period of at least 1 week. The sampling and measurement schedules for the scopolamine challenges were identical for both studies. The measurements were performed during 36 hours treatments periods with 11 measurement time-points from baseline (pre-dose) to 8.5 hrs after scopolamine (or placebo) administration.

Trial 3 evaluated the effect of a novel a_7 nicotinic acetylcholine receptor agonist (a_7 nAChR) during a scopolamine challenge test. The study recruited 35 subjects between 65 and 85 years. All subjects received 0.3 mg scopolamine (IV) in 15 minutes. Neurophysiological tests were measured with 8 measurement times from twice at baseline (-1 day) to 6 h after scopolamine administration (open-label). A detailed description of the neurophysiologic tests can be found elsewhere (Alvarez-Jimenez *et al*, 2016; Liem-Moolenaar *et al*, 2011).

Trial 4 consisted of 40 mild to moderate AD patients who were recently diagnosed with 'probable AD' (according to NINCDS-ADRDA), mild to moderate severity of dementia (according to Clinical Dementia Rating Score, CDR of 0.5-2) and a Mini-Mental State Exam score of 18–26. Here, we used eyes-closed rest EEG recordings obtained in the baseline before the administration of an investigational drug.

EEG RECORDINGS AND PRE-PROCESSING

EEG recordings were made using silver chloride electrodes fixed at FZ, CZ, PZ and OZ positions, with the same common reference electrode as for the eye movement registration (according to the international 10/20 system). Electrode resistances were kept below 5 kΩ. EEG signals were obtained from leads Fz-Cz and Pz-Oz and a separate channel to record eye movements (for artefacts). The signals were amplified by use of a Grass telefector (F-15EB/B1) and a 15LT series Amplifier Systems (Grass-Telefactor) with a time constant of 0.3 s and a low-pass filter at 100 Hz. The duration of the recordings was 64 s (Zuurman *et al*, 2008). Sampling frequency was 64768 Hz, afterwards down-sampled to 1012 Hz for the analysis. The ongoing EEG was visually inspected in windows of 10 s and sharp transient artefacts were cut out, as well as eye movement and muscle artefacts. Noisy channels were excluded from the subsequent analysis.

For the EEG analysis, the Neurophysiological Biomarker Toolbox (NBT) (http://www.nbtwiki.net/) (Hardstone *et al*, 2012) was used to calculate the biomarkers and custom made scripts were integrated with the NBT analysis pipeline for advanced statistics, employing data mining algorithms to combine the information from multiple biomarkers. We employed biomarker algorithms in order to extract both temporal and spectral information from the EEG signals in the classical frequency bands: δ (1–4 Hz), ϑ (4–8 Hz), *a* (8–13 Hz), and *β* (13–30 Hz). The power in these frequency bands was computed using the Welch method with a 4096-point Hamming window and a frequency resolution of 0.25 Hz. The relative power was calculated by dividing the absolute power in each frequency band with the integrated power in the range 1–45 Hz. The central frequency, *fc*, and bandwidth, *fσ* (Vural and Yildiz, 2010), were computed according to the formulas:

$$f_c = \frac{\Sigma_{f=fL}^{fH} fP(f)}{\Sigma_{f=fL}^{fH} fP(f)} \qquad f_\sigma = \sqrt{\frac{\Sigma_{f=fL}^{fH} (f-f_c)^2 P(f)}{\Sigma_{f=fL}^{fH} fP(f)}}$$

where *fL* and *fH* represent the lowest and highest frequency that defines a given frequency band, and *P(f)* denotes the power at frequency *f*. Thus, the central frequency biomarker provides information about where the power is concentrated in a given frequency band, whereas the bandwidth provides information about how much the power is spread out around the central frequency.

The amplitude envelope was extracted using the Hilbert transform and analyzed for long-range temporal correlations of the power-law form using detrended fluctuation analysis (DFA) (Hardstone *et al*, 2012; Linkenkaer-Hansen *et al*, 2001; Peng *et al*, 1995). If a sequence of events has a non-random temporal structure with slowly decaying autocorrelations, DFA can quantify how slowly these correlations decay as indexed by the DFA power-law exponent. Signals were filtered using a FIR filter with a Hamming window with a length corresponding to two *f1* Hz cycles for frequency band [*f1,f2*]. To minimize temporal correlations introduced by the FIR filter, DFA was fitted in the interval from 4 to 20 seconds for δ and ϑ band, from 2 to 20 seconds for *a* and 1 to 20 seconds for the *β* band. The oscillation burst lifetime was used to quantify differences in amplitude dynamics of oscillations on short to intermediate time scales (< 1 s)(Montez *et al*, 2009; Poil *et al*, 2011). We used a threshold at the median of the amplitude envelope and defined the beginning and the end of an oscillation burst as the time points of crossing this threshold. The duration of oscillation bursts was calculated by taking the 95TH percentile of all durations measured within each channel, which we refer to as the 'oscillation burst lifetime' biomarker. In total, 20 biomarkers were extracted from each EEG signal. Each of the biomarkers was computed over two bipolar channels (Fz-Cz and Pz-Oz) resulting in a total of 40 features for classification analysis.

STATISTICAL ANALYSIS

Machine learning techniques were used to find the biomarkers that best distinguished the peak effect of scopolamine from the baseline recording or that best distinguished AD patients from healthy controls. From time-dependent curves of EEG biomarkers (Figure 7.2), we evaluated 1.5 h after administration of scopolamine as the peak for most EEG biomarkers – in agreement with the peak drug effect (τ_max) time point according to the cognitive measurements (Alvarez-Jimenez *et al*, 2016; Liem-Moolenaar *et al*, 2011); therefore, we performed classification on the EEG recorded at baseline and 1.5 h after administration of scopolamine for the development of the mAChR index. For the AD index, we used pre-intervention baseline recordings of AD patients and healthy controls.

A feature matrix was built from the EEG biomarkers – in the form #features × #samples – with the aim of identifying sets of biomarkers that were more discriminative between the two groups than each individual biomarker. Feature selection and classification were performed via the classical machine learning procedure steps: training and testing. In the training phase, the index was developed by applying the feature-selection algorithm to training data and in the test phase, the index was applied to predict the class membership

on the test data. The features used for machine learning were z-scored EEG biomarker values. To avoid introducing future information into the classifier, we normalized both the training and the test data by subtracting the mean and dividing by the standard deviation of biomarker values from the training data only.

Indices were identified by applying the classification algorithm to the whole dataset (Trials 1 and 2 for mAChR; Trials 3 and 4 for the AD index); however, cross-validation was used to evaluate the stability of the result, i.e., classification with 100 different splits of the data into training and test sets were performed to obtain the mean and standard deviation of the classification performance, which provides an estimate of the classification performance on an 'unknown' sample (Witten *et al*, 2011). To this end, we used the cross-validation with 70/30% random splitting, i.e., from a random permutation of the subjects, 70% were used for training and 30% for testing. The training set consisted of 115 EEG recordings, tested on 48 recordings for the mAChR index (Trial 1 and 2). The total number of recordings is twice the number of subjects: per subject, the baseline EEG recording was used as the first sample and the peak drug effect recording as the second sample. For the AD index, the training and test set consisted of 53 and 22 recordings (and subjects), respectively (Trial 3 and 4).

ELASTIC NET LOGISTIC REGRESSION

Because of the correlation between some of the features, we performed feature selection and classification using the elastic net (Zou and Hastie, 2005), with sparsity and grouping of correlated features as properties. Elastic net is a feature selection and classification method based on regularized logistic regression that bridges the gap between lasso (Tibshirani, 2011) and ridge regression (Hoerl and Kennard, 1970) by combining their penalties and optimizing the number of features included in the integrated index through minimizing the function:

$$L(\lambda_1, \lambda_2, \beta) = y - X\beta^2 + \lambda_1\beta_1 + \lambda_2\beta_2^2$$

where X is the feature matrix, y is the response vector (the labels) β the weights, and λ_1 and λ_2 coefficients determining the influence of the L_1 and L_2 norm penalties, respectively. The first term is similar to logistic regression while the second and third terms form the elastic net penalty function. If we denote: $a=\lambda_2\lambda_1+\lambda_2$, then the elastic net penalty can be rewritten as $(1-a)\beta_1+a\beta_2^2$, where a acts as the balancing term between the L_1 and L_2 norm penalties. We optimized a in random-splitting cross-validation procedure and found the best classification performance with $a = 0.5$ (results not shown).

By minimizing the L-function, we obtain the set of n selected features corresponding to the ones with highest β values. If p is the probability that an EEG recording belongs to the peak scopolamine condition, then the odds ratio is $p(1-p)$, which is the ratio of the probability of peak scopolamine to the probability of baseline recording. Logistic regression models the log odds ratio as a linear combination of the independent variables, via this equation:

$$\ln\left(\frac{p}{1-p}\right) = \beta_0 + \beta_1 f_1 + \dots + \beta_n f_n$$

where f_1 are the features and β_1 the associated weights. The log odds can be transformed back to probabilities as:

$$p(t) = \frac{1}{1 + exp(-t)} \qquad\qquad t = \beta_0 + \beta_1 f_1 + \dots + \beta_n f_n$$

The size of the final set of selected features is estimated as the one that gives the maximum classification performance on the training set, while keeping the feature set as small as possible. To obtain this set, we compared the accuracy of classifiers using the k best β-s, with k ranging from 1 to the number of features n and selected the smallest feature set with optimal performance.

CLASSIFICATION OUTCOME EVALUATION

Elastic net logistic regression algorithm was used for developing two integrated indices: 1) The mAChR index, which is classifying whether an EEG was recorded during the baseline or when scopolamine has been administered; 2) The AD index, which is classifying whether an EEG was recorded from a healthy elderly or an AD patient. To evaluate the classification

performance of the indices we used four different measures. In the case of the mAChR index, they are defined as:

- Accuracy (ACC): (number of correctly classified peak scopolamine and baseline recordings)/(total number of recordings).
- Sensitivity (SE): (number of correctly classified scopolamine recordings)/(number of scopolamine recordings).
- Specificity (SP): (number of correctly classified baseline recordings)/(number of baseline recordings).
- Precision (PPV): (number of correctly classified scopolamine recordings)/(number of recordings classified as scopolamine).
- Area Under Curve (AUC): area under the Receiver Operating Characteristic (ROC) curve, which plots the true positive rate (SE) against the true negative rate (1-SP) as the discrimination threshold of the classifier is varied. A higher AUC means better classification performance.
- Analogous definitions apply for the classification performance of the AD index.

<div align="center">

RESULTS

SCOPOLAMINE AFFECTS BOTH SPECTRAL AND TEMPORAL DYNAMICS OF THE EEG

</div>

To gain a comprehensive understanding of the effects of scopolamine on the EEG, we employed biomarker algorithms characterizing spectral content as well as temporal dynamics of neuronal oscillations. The spectral content was estimated using power spectrum analysis of the broadband EEG signals (Figure 7.1). The short-time scale temporal structure of narrow-band oscillations was quantified by extracting the amplitude envelope and applying oscillation-bursts lifetime analysis (Figure 7.1), whereas temporal dynamics on longer time scales was quantified using DFA (Figure 7.1).

To examine the effects of scopolamine administration compared to placebo, we quantified these differences systematically at 11 time points from 30 minutes before to 8.5 hours after scopolamine and placebo administration. In Figure 7.2, we display the results as time-dependent biomarker curves of relative power, central frequency, bandwidth, oscillation-burst lifetime, and DFA in the columns and the frequency bands in the rows. A significant effect of scopolamine compared to placebo was observed for several biomarkers (Wilcoxon rank sum test at 1.5 h after administration, Bonferroni corrected). Despite all of these robust effects, if biomarkers carry complementary information about scopolamine-induced EEG changes, then it may be possible to combine this information into a more sensitive measure of the anticholinergic effect compared to using any of the individual biomarkers.

INTEGRATING BIOMARKERS ENHANCES CLASSIFICATION

We used machine-learning techniques to find the biomarkers that best distinguish the baseline from the peak scopolamine condition. In order to do this, we performed classification on the baseline recording and the EEG recorded 1.5 h after administration of scopolamine (Figure 7.2). The baseline was used as opposed to the placebo condition to eliminate variation between days.

An initial integrated index was developed using elastic net on the data from healthy subjects ($n = 83$ males, Trial 1 and 2, see Methods) that received scopolamine, while allowing a fraction – determined by the algorithm – of the 40 available biomarkers to be included. Subsequently, to simplify the composition of the index, biomarkers with non-zero weights were sorted by decreasing absolute weight and added incrementally in that order (i.e., starting from an empty set, we added the biomarker with the largest absolute weight etc.) to evaluate the gain of including each subsequent biomarker to the classifier. Accuracy and AUC increased with the number of features included in the index up until a maximum performance was reached (Figure 7.3). We defined the optimal index to be the one with the smallest number of features for which the average of all performance measures had saturated. We estimated this number to be 14 (Figure 7.3) according to the 'elbow' method (Ketchen and Shook, 1996); together, this set of 14 biomarkers and their associated weights make up the integrated mAChR index (Figure 7.3).

The mAChR index had excellent performance when training and testing on the same data (accuracy 95%, sensitivity 96%, specificity 93%, precision

93% and area under curve 0.98), and much higher than the single-best biomarker, which was relative delta power (Figure 7.3). Accordingly, the difference between the baseline predicted group and the peak scopolamine predicted group (Figure 7.3) was much more pronounced for the mAChR index ($p = 2^*10^{-26}$, Wilcoxon rank sum test) than for relative delta ($p = 6^*10^{-16}$). To obtain a more accurate estimate of the classification performance, we used cross-validation. The difference in performance per cross-validation was due to different subsets of subjects used for training and testing in each iteration, resulting in slightly different biomarker selections and weights. Cross-validation on these two datasets (Figure 7.3) resulted in an accuracy of $90 \pm 2\%$, sensitivity of $92 \pm 4\%$, specificity of $88 \pm 4\%$ and precision of $88 \pm 3\%$, which is still very high and significantly higher than using just relative delta: accuracy of $79 \pm 2\%$, sensitivity of $79 \pm 4\%$, specificity of $83 \pm 4\%$ and precision of $81 \pm 3\%$ ($p = 9^*10^{-29}$ for accuracy, Wilcoxon rank sum test). Interestingly, the difference between the baseline predicted and scopolamine predicted groups was also more significant for the mAChR index ($p = 9^*10^{-10}$, Wilcoxon rank sum test) than for relative delta ($p = 0.02$) when tested at washout – 8.5 h after scopolamine administration (Figure 7.3).

THE mAChR INDEX IS ROBUST AND GENERALIZABLE

Test-retest stability is an important quality of a biomarker. We therefore compared the mAChR index scores of baseline recordings from two separate days in 75 subjects (Trial 1 and 2) and observed a strong correlation of 0.64 (Spearman correlation, $p = 2.5^*10^{-10}$, Figure 7.3). To further demonstrate the generalizability of the mAChR index, we applied it to an independent cohort of healthy elderly subjects (Trial 3, see Methods) receiving a similar scopolamine intervention. Interestingly, in spite of the difference between the age groups in Trials 1–2 and 3, we observed an index performance very close to the cross-validation on the adult cohort (Figure 7.4; accuracy 87%, sensitivity 83%, specificity 91% and precision 91%). Importantly, the index also generalized to the other measurement time points both for Trials 1, 2 and 3 (Figure 7.4).

SCOPOLAMINE IS A VALID MODEL OF AD PATHOPHYSIOLOGY

To test the validity of scopolamine as a model for the cholinergic dysfunction that occurs in AD, we next developed an AD index. Using the patients with mild to moderate AD (Trial 4) and the age-matched healthy elderly subjects (Trial 3), we derived an AD index consisting of 12 biomarkers (Figure 7.5), of which 5 are the same as those in the mAChR index. The AD index performed with an accuracy of 92%, sensitivity 87%, specificity 97% and precision 97% when training and testing on the same data (Figure 7.5). Cross-validated, the respective performances were $73 \pm 6\%$, $73 \pm 9\%$, $70 \pm 10\%$ and $75 \pm 7\%$. Next, we investigated the relation of the AD index to the mAChR index, comparing their abilities to discriminate healthy elderly subjects from patients with mild to moderate AD, or discriminate baseline from peak scopolamine. Applying the mAChR index on healthy elderly and AD patients, we observed that it was able to discriminate them, with an accuracy of 62%, sensitivity 35%, specificity 91% and precision 81% (Figure 7.5). The separation was better when applying the AD index on subjects before and after scopolamine intervention, with accuracy 72%, sensitivity 89%, specificity 54% and precision 66%. Taken together our results show that the mAChR index captures cholinergic dysfunction that occurs in AD. This is reflected by several biomarkers shared between the mAChR and the AD index, as well as the mutual ability to distinguish subjects with AD or subjects given scopolamine, respectively. Also, the good performance of the AD index in discriminating healthy elderly from AD patients further demonstrates the value of multi-biomarker classification schemes.

DISCUSSION

Resting-state EEG signals are complex and information rich (Linkenkaer-Hansen *et al*, 2001). A variety of spectral, spatial and temporal biomarker algorithms have been used to uncover brain electrophysiological changes in disease or with pharmacological intervention (Arns and Olbrich, 2014; Montez *et al*, 2009; Mucci *et al*, 2006); however, they all have too low sensitivity and specificity to become standard tools in hospitals and

clinical trials (Ommundsen *et al*, 2011; van Straaten *et al*, 2014). To address this problem, we tested whether extensive characterization of EEG using multiple biomarkers and subsequent application of machine learning could improve the accuracy of classifying disease state or drug intervention. We developed a mAChR index with superior sensitivity and specificity to the complex structure of the EEG changes induced by scopolamine intervention compared to any single biomarker. The enhanced accuracy could be of great value in evaluating the efficacy of drugs that aim to induce effects opposite to scopolamine, e.g., for the treatment of AD and schizophrenia-related cognitive impairment. We believe our methodological approach could prove invaluable in a wide range of challenge tests used in CNS drug development.

SCOPOLAMINE AFFECTS VARIOUS PROPERTIES OF NEURONAL OSCILLATIONS

Scopolamine is known to decrease alpha power and increase relative delta and theta power, mainly in posterior regions (Kikuchi *et al*, 1999; Liem-Moolenaar *et al*, 2011; Sannita *et al*, 1987). These EEG changes are hallmarks of cognitive impairment associated with AD (Bennys *et al*, 2001; Dauwels *et al*, 2010a; Jeong, 2004) and also observed in our healthy subjects after scopolamine administration (Figure 7.2). Other biomarkers affected by scopolamine included the oscillation burst lifetime biomarker, which decreased in the alpha band (Figure 7.1) and increased in the theta band (Figure 7.2) as observed also in early-stage AD (Montez *et al*, 2009). Scopolamine produced an increase in DFA in all frequency bands, albeit this effect was only sufficiently strong in the beta band for inclusion in the mAChR index (Figure 7.1 and Figure 7.2). The mAChR index also comprised the central frequency effects of a decrease in the theta band and an increase in the alpha and beta bands (Figure 7.2). Changes in the central frequency and bandwidth were correlated, decreasing in the theta band and increasing in alpha and beta bands. Larger bandwidth could be associated with less frequency stability of alpha and beta oscillations, which has previously been linked to a less efficient working memory (Kopell et al, 2011).

MACHINE LEARNING FOR MORE ACCURATE MEASURES OF PATHOPHYSIOLOGY

A similar analysis using machine learning for classifying scopolamine effects on the EEG has been developed in the past (Johannsson et al, 2015); however, with different features and analysis methods used and without reporting the classification performance of the index; therefore, it cannot readily be compared with our findings. Our cross-validation (training and testing on different data) resulted in a remarkable performance (Figure 7.3). Importantly, the test-retest reliability of the mAChR index across two baseline recordings was very high (Figure 7.3), and validation on an independent set of data confirmed that the index generalizes to new cohorts (Figure 7.4). Interestingly, when classifying on the washout period, classification with the mAChR index was highly significant, whereas that of the single-best biomarker was only marginally significant (Figure 7.3), suggesting that clinical situations with many more subtle drug effects will gain substantially from the proposed machine learning and data-integration approach. This is particularly useful in view of the fact that acute pharmacodynamics effects of pro-cognitive, cholinergic compounds are often difficult to measure in healthy subjects or patients with AD (Balsters *et al*, 2011; Beglinger *et al*, 2004, 2005; Nathan *et al*, 2001).

To examine the validity of scopolamine as a model of AD pathophysiology, we applied the mAChR index to healthy elderly controls and patients with AD. We also derived an AD index to test whether scopolamine-induced EEG changes resemble those of AD. Applying the mAChR index to AD patients and controls we observed that it indeed showed an effect (Figure 7.5); however, it discriminated less accurately than the AD index and with a shift in the classification threshold. According to the mAChR index, some AD patients were misclassified as healthy elderly, presumably because the EEG is affected more strongly by scopolamine than mild (or moderate) AD. Nonetheless, because the differences were in the same direction, applying the AD index to the subjects on scopolamine resulted in a much better separation (Figure 7.5). The misclassification here was opposite: a few baseline recordings were predicted as scopolamine, because the differences between healthy elderly and AD are weaker and, therefore, the separation threshold for the AD index is

lower. Together, this suggests that scopolamine is a good cognitive impairment model for AD, mimicking the changes seen in AD patients; however, with a difference in the magnitude of effects. Nicotinic blockade added to the muscarinic anticholinergic effects might better resemble changes reflected in both indices and might further explain the difference observed between AD and scopolamine peak effects (Ellis *et al*, 2006; Erskine *et al*, 2004; Gitelman and Prohovnik, 1992; Little *et al*, 1998).

MACHR INDEX – POTENTIAL AS A CLINICAL EEG TOOL AND FUTURE DEVELOPMENTS

Integrating information from multiple EEG biomarkers has an advantage over the standard power spectrum, because of the often subtle changes from baseline and the considerable inter-individual variability at baseline for EEG and cognitive tests. This approach also reduces the multiple-comparisons problem when analyzing several EEG biomarkers in clinical trials. A specific mAChR index may help to quantify effects of pro-cognitive cholinergic compounds, and muscarinic agonists in particular. Reversal of detrimental effects induced by scopolamine on cognitive performance has been demonstrated in humans with donepezil (Snyder *et al*, 2005; Thomas *et al*, 2008) and galantamine (Baraka and Harik, 1977) – two cholinesterase inhibitors that increase acetylcholine in the synaptic cleft and prescribed for the symptomatic treatment of patients with AD. Further research to develop a nicotinic cholinergic index would also be an important tool in drug development as nicotinic reversal has also been successfully reported (Woodruff-Pak *et al*, 2003), therefore an index for nicotinic antagonists could provide a useful non-invasive method to monitor the effects of an important class of drugs.

Furthermore, while improvement of cognitive functions is difficult to quantify in healthy subjects (Beglinger *et al*, 2004, 2005), administration of the agonists may induce changes in the mAChR index that might not be quantifiable with other cognitive tests without the use of a pharmacologic challenge test (Cohen, 2010). Therefore, a more accurate measure of the EEG effects of scopolamine and of cholinergic compounds may result in superior

detection of pharmacological (scopolamine reversing) effects. This is very important for drug development, both in terms of proof-of-pharmacology and dose finding. Showing reversal of scopolamine effects by cholinergic compounds (even those proven to be effective in the clinic) is difficult, but this method holds potential: it improves detection of muscarinic anticholinergic EEG effects, so we can expect it to be beneficial at showing the reversal of those effects as well. Moreover, this method may also help to detect cholinergic effects in healthy subjects (or AD patients) who have not been given the scopolamine challenge.

In conclusion, scopolamine effects on the EEG are clearly present and the spectral ones are well known; however, the mAChR index also accommodates the temporal dynamics to provide deeper insight into the brain's cholinergic electrophysiology. The index serves as a sensitive biomarker to detect the effect of scopolamine in a dose-dependent manner as well as provide evidence for drug penetration and, therefore, holds potential for being used in experimental pharmacology.

REFERENCES

Agnoli A, Martucci N, Manna V, Conti L, Fioravanti M (1983). Effect of cholinergic and anticholinergic drugs on short-term memory in Alzheimer's dementia: a neuropsychological and computerized electroencephalographic study. *Clin Neuropharmacol* 6: 311–23.

Ali-Melkkilä T, Kanto J, Iisalo E (1993). Pharmacokinetics and related pharmacodynamics of anticholinergic drugs. *Acta Anaesthesiol Scand* 37: 633–42.

Alvarez-Jimenez R, Groeneveld GJ, Gerven JMA van, Goulooze SC, Baakman AC, Hay JL, *et al* (2016). Model-based exposure-response analysis to quantify age related differences in the response to scopolamine in healthy subjects. *Br J Clin Pharmacol* 82: 1011–21.

Arns M, Olbrich S (2014). Personalized Medicine in ADHD and Depression: Use of Pharmaco-EEG. *Curr Top Behav Neurosci* 21: 345–70.

Babiloni C, Binetti G, Cassetta E, Cerboneschi D, Dal Forno G, Percio C Del, *et al* (2004). Mapping distributed sources of cortical rhythms in mild Alzheimer's disease. A multicentric EEG study. *Neuroimage* 22: 57–67.

Balsters JH, O'Connell RG, Martin MP, Galli A, Cassidy SM, Kilcullen SM, *et al* (2011). Donepezil impairs memory in healthy older subjects: behavioural, EEG and simultaneous EEG/fMRI biomarkers. *PLoS One* 6: e24126.

Baraka A, Harik S (1977). Reversal of central anticholinergic syndrome by galanthamine. *JAMA* 238: 2293–4.

Beglinger LJ, Gaydos BL, Kareken DA, Tangphao-Daniels O, Siemers ER, Mohs RC (2004). Neuropsychological test performance in healthy volunteers before and after donepezil administration. *J Psychopharmacol* 18: 102–8.

Beglinger LJ, Tangphao-Daniels O, Kareken DA, Zhang L, Mohs R, Siemers ER (2005). Neuropsychological test performance in healthy elderly volunteers before and after donepezil administration: a randomized, controlled study. *J Clin Psychopharmacol* 25: 159–65.

Bennys K, Rondouin G, Vergnes C, Touchon J (2001). Diagnostic value of quantitative EEG in Alzheimer's disease. *Neurophysiol Clin* 31: 153–60.

Blennow K, Leon MJ de, Zetterberg H (2006). Alzheimer's disease. *Lancet* 368: 387–403.

Broks P, Preston GC, Traub M, Poppleton P, Ward C, Stahl SM (1988). Modelling dementia: effects of scopolamine on memory and attention. *Neuropsychologia* 26: 685–700.

Cho W, Maruff P, Connell J, Gargano C, Calder N, Doran S, *et al* (2011). Additive effects of a cholinesterase inhibitor and a histamine inverse agonist on scopolamine deficits in humans. *Psychopharmacology (Berl)* 218: 513–24.

Citron M (2010). Alzheimer's disease: strategies for disease modification. *Nat Rev Drug Discov* 9: 387–98.

Cohen AF (2010). Developing drug prototypes: pharmacology replaces safety and tolerability? *Nat Rev Drug Discov* 9: 856–65.

Dauwels J, Vialatte F, Cichocki A (2010a). Diagnosis of Alzheimer's disease from EEG signals: where are we standing? *Curr Alzheimer Res* 7: 487–505.

Dauwels J, Vialatte F, Musha T, Cichocki A (2010b). A comparative study of synchrony measures for the early diagnosis of Alzheimer's disease based on EEG. *Neuroimage* 49: 668–93.

Ebert U, Siepmann M, Oertel R, Wesnes K a, Kirch W (1998). Pharmacokinetics and pharmacodynamics of scopolamine after subcutaneous administration. *J Clin Pharmacol* 38: 720–6.

Ellis JR, Ellis K a, Bartholomeusz CF, Harrison BJ, Wesnes K a, Erskine FF, *et al* (2006). Muscarinic and nicotinic receptors synergistically modulate working memory and attention in humans. *Int J Neuropsychopharmacol* 9: 175–89.

Erskine FF, Ellis JR, Ellis KA, Stuber E, Hogan K, Miller V, *et al* (2004). Evidence for synergistic modulation of early information processing by nicotinic and muscarinic receptors in humans. *Hum Psychopharmacol* 19: 503–9.

Frank R, Hargreaves R (2003). Clinical biomarkers in drug discovery and development. *Nat Rev Drug Discov* 2: 566–80.

Franz VH, Loftus GR (2012). Standard errors and confidence intervals in within-subjects designs: generalizing Loftus and Masson (1994) and avoiding the biases of alternative accounts. *Psychon Bull Rev* 19: 395–404.

Gitelman DR, Prohovnik I (1992). Muscarinic and nicotinic contributions to cognitive function and cortical blood flow. *Neurobiol Aging* 13: 313–318.

Golde TE (2016). Overcoming translational barriers impeding development of Alzheimer's disease modifying therapies. *J Neurochem* doi:10.1111/jnc.13583.

Hardstone R, Poil S-S, Schiavone G, Jansen R, Nikulin V V., Mansvelder HD, *et al* (2012). Detrended fluctuation analysis: a scale-free view on neuronal oscillations. *Front Physiol* 3: 450.

Hoerl AE, Kennard RW (1970). Ridge Regression: Biased Estimation for Nonorthogonal Problems. *Technometrics* 12: 55–67.

Jeong J (2004). EEG dynamics in patients with Alzheimer's disease. *Clin Neurophysiol* 115: 1490–505.

Johannsson M, Snaedal J, Johannesson GH, Gudmundsson TE, Johnsen K (2015). The Acetylcholine Index: An Electroencephalographic Marker of Cholinergic Activity in the Living Human Brain Applied to Alzheimer's Disease and Other Dementias. *Dement Geriatr Cogn Disord* 39: 132–142.

Jones RW, Wesnes K a, Kirby J (1991). Effects of NMDA modulation in scopolamine dementia. *Ann N Y Acad Sci* 640: 241–4.

Ketchen DJ, Shook CL (1996). *The application of cluster analysis in strategic management research: An analysis and critique..*

Khodayari-Rostamabad A, Hasey GM, Maccrimmon DJ, Reilly JP, Bruin H de (2010). A pilot study to determine whether machine learning methodologies using pre-treatment electroencephalography can predict the symptomatic response to clozapine therapy. *Clin Neurophysiol* 121: 1998–2006.

Kikuchi M, Wada Y, Nanbu Y, Nakajima A, Tachibana H, Takeda T, *et al* (1999). EEG Changes following Scopolamine Administration in Healthy Subjects. *Neuropsychobiology* 39: 219–226.

Klinkenberg I, Blokland A (2010). The validity of scopolamine as a pharmacological model for cognitive impairment: a review of animal behavioral studies. *Neurosci Biobehav Rev* 34: 1307–50.

Kopell N, Whittington MA, Kramer MA (2011). Neuronal assembly dynamics in the beta1 frequency range permits short-term memory. *Proc Natl Acad Sci U S A* 108: 3779–84.

Lehmann C, Koenig T, Jelic V, Prichep L, John RE, Wahlund L-O, *et al* (2007). Application and comparison of classification algorithms for recognition of Alzheimer's disease in electrical brain activity (EEG). *J Neurosci Methods* 161: 342–50.

Leiser SC, Dunlop J, Bowlby MR, Devilbiss DM (2011). Aligning strategies for using EEG as a surrogate biomarker: A review of preclinical and clinical research. *Biochem Pharmacol* 81: 1408–1421.

Liem-Moolenaar M, Boer P de, Timmers M, Schoemaker RC, Hasselt JGC van, Schmidt S, *et al* (2011). Pharmacokinetic-pharmacodynamic relationships of central nervous system effects of scopolamine in healthy subjects. *Br J Clin Pharmacol* 71: 886–98.

Liem-Moolenaar M, Zoethout RWM, Boer P de, Schmidt M, Kam ML de, Cohen AF, *et al* (2010a). The effects of the glycine reuptake inhibitor R213129 on the central nervous system and on scopolamine-induced impairments in psychomotor and cognitive function in healthy subjects. *J Psychopharmacol* 24: 1671–9.

Liem-Moolenaar M, Zoethout RWM, Boer P de, Schmidt M, Kam ML de, Cohen AF, *et al* (2010b). The effects of a glycine reuptake inhibitor R231857 on the central nervous system and on scopolamine-induced impairments in cognitive and psychomotor function in healthy subjects. *J Psychopharmacol* 24: 1681–7.

Linkenkaer-Hansen K, Nikouline V V., Palva JM, Ilmoniemi RJ (2001). Long-range temporal correlations and scaling behavior in human brain oscillations. *J Neurosci* 21: 1370–7.

Little JT, Johnson DN, Minichiello M, Weingartner H, Sunderland T (1998). Combined nicotinic and muscarinic blockade in elderly normal volunteers: cognitive, behavioral, and physiologic responses. *Neuropsychopharmacology* 19: 60–9.

Lopes da Silva F (2013). EEG and MEG: relevance to neuroscience. *Neuron* 80: 1112–28.

Montez T, Poil S-S, Jones BF, Manshanden I, Verbunt JPA, Dijk BW van, *et al* (2009). Altered temporal correlations in parietal alpha and prefrontal theta oscillations in early-stage Alzheimer disease. *Proc Natl Acad Sci U S A* 106: 1614–1619.

Mucci A, Volpe U, Merlotti E, Bucci P, Galderisi S (2006). Pharmaco-EEG in psychiatry. *Clin EEG Neurosci* 37: 81–98.

Nathan PJ, Baker A, Carr E, Earle J, Jones M, Nieciecki M, *et al* (2001). Cholinergic modulation of cognitive function in healthy subjects: acute effects of donepezil, a cholinesterase inhibitor. *Hum Psychopharmacol Clin Exp* 16: 481–483.

Oertel W, Schulz JB (2016). Current and experimental treatments of Parkinson disease: A guide for neuroscientists. *J Neurochem* doi:10.1111/jnc.13750.

Ommundsen N, Engedal K, Øksengård AR (2011). Validity of the quantitative EEG statistical pattern recognition method in diagnosing Alzheimer's disease. *Dement Geriatr Cogn Disord* 31: 195–201.

Osipova D, Ahveninen J, Jensen O, Ylikoski A, Pekkonen E (2005). Altered generation of spontaneous oscillations in Alzheimer's disease. *Neuroimage* 27: 835–41.

Peng CK, Havlin S, Stanley HE, Goldberger AL (1995). Quantification of scaling exponents and crossover phenomena in nonstationary heartbeat time series. *Chaos* 5: 82–7.

Poil S-S, Haan W de, Flier WM van der, Mansvelder HD, Scheltens P, Linkenkaer-Hansen K (2013). Integrative EEG biomarkers predict progression to Alzheimer's disease at the MCI stage. *Front Aging Neurosci* 5: 58.

Poil S-S, Jansen R, Aerde K van, Timmerman J, Brussaard AB, Mansvelder HD, *et al* (2011). Fast network oscillations in vitro exhibit a slow decay of temporal auto-correlations. *Eur J Neurosci* 34: 394–403.

Preda L, Alberoni M, Bressi S, Cattaneo C, Parini J, Canal N, *et al* (1993). Effects of acute doses of oxiracetam in the scopolamine model of human amnesia. *Psychopharmacology (Berl)* 110: 421–6.

Prohovnik I, Arnold SE, Smith G, Lucas LR (1997). Physostigmine reversal of scopolamine-induced hypofrontality. *J Cereb Blood Flow Metab* 17: 220–8.

Sankari Z, Adeli H, Adeli A (2012). Wavelet coherence model for diagnosis of Alzheimer disease. *Clin EEG Neurosci* 43: 268–78.

Sannita WG, Maggi L, Rosadini G (1987). *Effects of scopolamine (0.25-0.75 mg i.m.) on the quantitative EEG and the neuropsychological status of healthy volunteers. Neuropsychobiology* 17:.

Schyf CJ Van der, Geldenhuys WJ (2011). Multimodal drugs and their future for Alzheimer's and Parkinson's disease. *Int Rev Neurobiol* 100: 107–25.

Siegfried KR (1993). Pharmacodynamic and early clinical studies with velnacrine. *Acta Neurol Scand Suppl* **149**: 26–8.

Snyder PJ, Bednar MM, Cromer JR, Maruff P (2005). Reversal of scopolamine-induced deficits with a single dose of donepezil, an acetylcholinesterase inhibitor. *Alzheimers Dement* **1**: 126–35.

Stam CJ, Made Y van der, Pijnenburg YAL, Scheltens P (2003). EEG synchronization in mild cognitive impairment and Alzheimer's disease. *Acta Neurol Scand* **108**: 90–6.

Straaten EC van, Scheltens P, Gouw AA, Stam CJ (2014). Eyes-closed task-free electroencephalography in clinical trials for Alzheimer's disease: an emerging method based upon brain dynamics. *Alzheimers Res Ther* **6**: 86.

Thomas E, Snyder PJ, Pietrzak RH, Jackson CE, Bednar M, Maruff P (2008). Specific impairments in visuospatial working and short-term memory following low-dose scopolamine challenge in healthy older adults. *Neuropsychologia* **46**: 2476–84.

Tibshirani R (2011). Regression shrinkage and selection via the lasso: A retrospective. *J R Stat Soc Ser B Stat Methodol* **73**: 273–282.

Vural C, Yildiz M (2010). Determination of sleep stage separation ability of features extracted from EEG signals using principle component analysis. *J Med Syst* **34**: 83–9.

Witten IH, Frank E, Hall M a. (2011). *Data Mining: Practical Machine Learning Tools and Techniques, Third Edition. Ann Phys (N Y)* **54**.

Woodruff-Pak DS, Vogel RW, Wenk GL (2003). Mecamylamine interactions with galantamine and donepezil: Effects on learning, acetylcholinesterase, and nicotinic acetylcholine receptors. *Neuroscience* **117**: 439–447.

Zou H, Hastie T (2005). Regularization and variable selection via the elastic net. *J R Stat Soc Ser B Stat Methodol* **67**: 301–320.

Zuurman L, Roy C, Schoemaker RC, Hazekamp A, Hartigh J den, Bender JC, *et al* (2008). Effect of intrapulmonary tetrahydrocannabinol administration in humans. *J Psychopharmacol* **22**: 707–716.

FIGURE 7.1-1   Spectral and temporal correlation biomarkers exhibit sensitivity to scopolamine administration.

A. EEG of a subject in the baseline (**blue**) and scopolamine (**red**) condition. **B**. Grand average normalized power spectra indicate large effects of scopolamine, most notably a reduction of power in the alpha and beta bands, and an increase of delta and theta power.
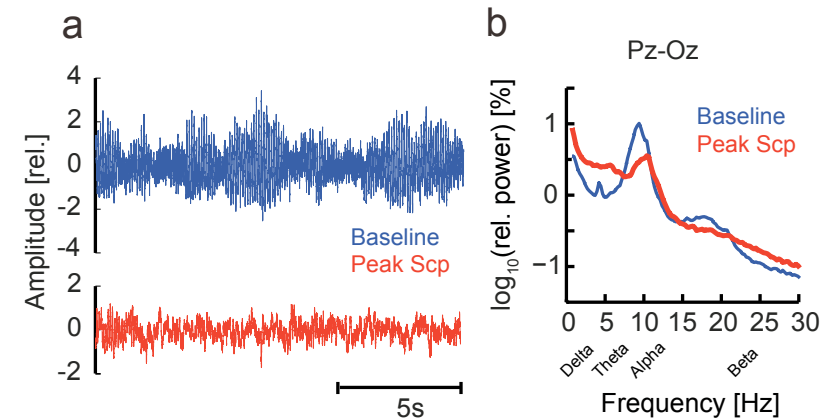
FIGURE 7.1-2   **Spectral and temporal correlation biomarkers exhibit sensitivity to scopolamine administration.**

c. Oscillation dynamics were studied by extracting the amplitude envelope from band-pass filtered data (e.g., the alpha band, **black**) using the Hilbert transform (**blue, red**) and a median-amplitude threshold to determine the onset and offset of a burst. **D**. A cumulative probability distribution of all oscillation bursts revealed a tendency towards longer alpha bursts in the baseline condition. **E**. Amplitude envelopes of beta oscillations (13–30 Hz) suggest a more complex temporal structure in the peak scopolamine (**red**) than in the baseline (**blue**) condition on time scales of seconds to tens of seconds. **F**. The long-time scale differences in beta oscillations are reflected in the grand average DFA showing larger scaling exponents for peak scopolamine (**red**) than for the baseline recording (**blue**). All figures were based on the pz-oz channel.
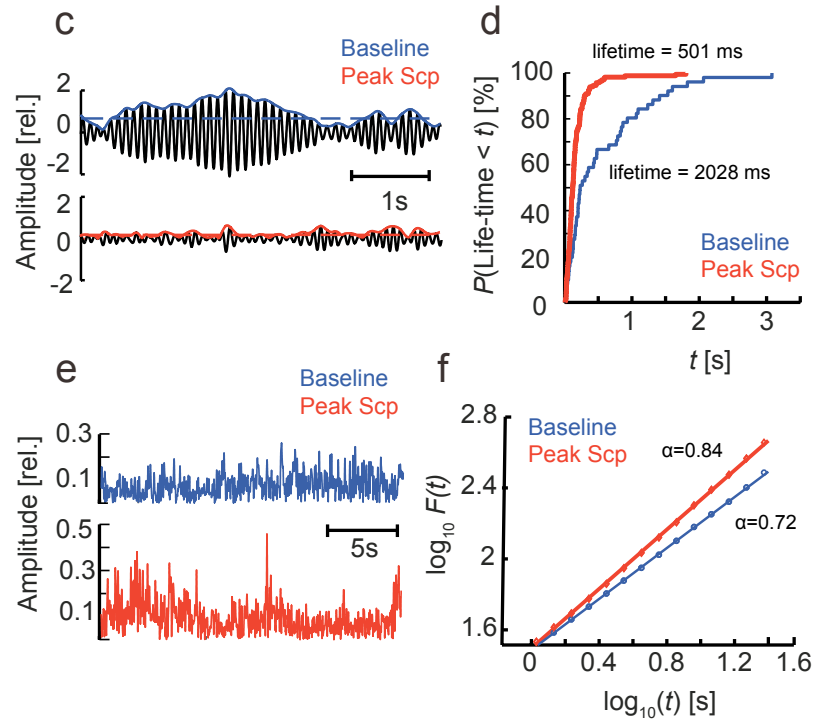

FIGURE 7.2   **Scopolamine affects many characteristics of the EEG.**

Time dependence of different EEG biomarkers (columns) and frequency bands (rows) for placebo (**black**) and scopolamine (**red**). All biomarkers are shown as averages over the 2 channels, except for relative power, for which the Fz-Cz and Pz-Oz channels are shown separately, because the effects in the delta and beta bands were opposite for the two derivatives. Sixteen biomarkers were significantly affected by scopolamine, with the peak effect occurring 1.5 h after administration.
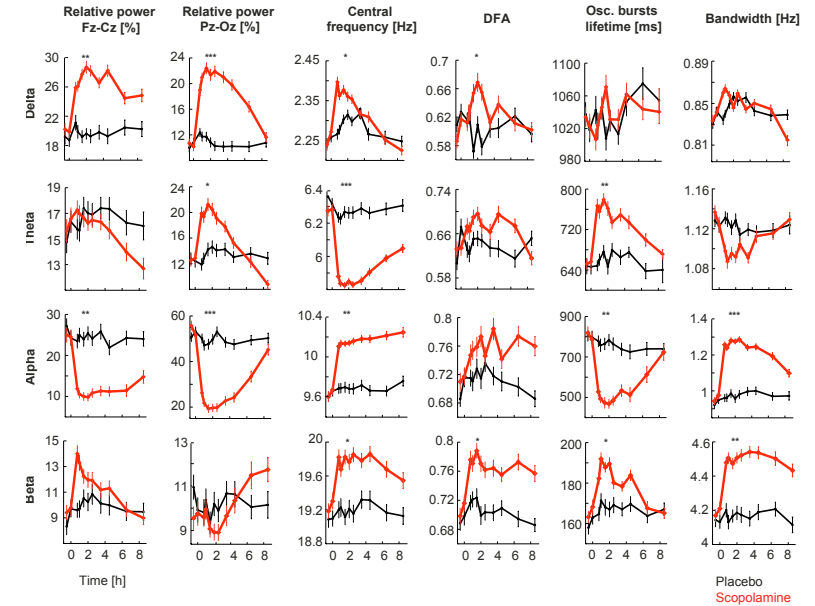
*Significance levels: * denotes p < 0.05, ** p < 10⁻⁵, *** p < 10⁻¹⁰*
Bonferroni corrected for multiple comparisons.

FIGURE 7.3-1   Enhanced detection of scopolamine-induced EEG changes using machine learning.

A. Classification performance increased with the number of features included in the integrated index. **B**. All of the biomarkers selected by elastic net logistic regression for inclusion in the integrated mAChR index differed significantly between baseline and peak scopolamine. Biomarkers are ordered by their absolute weights, decreasing clockwise from the top. Weights (β) are listed next to each biomarker in the legend (PO denotes Pz-Oz and FC denotes Fz-Cz). The values plotted on the spider plot are the z-score group means and standard error of the mean, normalized to $[0, 1]$ by subtracting the minimum across all biomarkers and dividing with the largest range present (i.e., the difference between the minimum and maximum value found for the biomarkers with the largest difference).
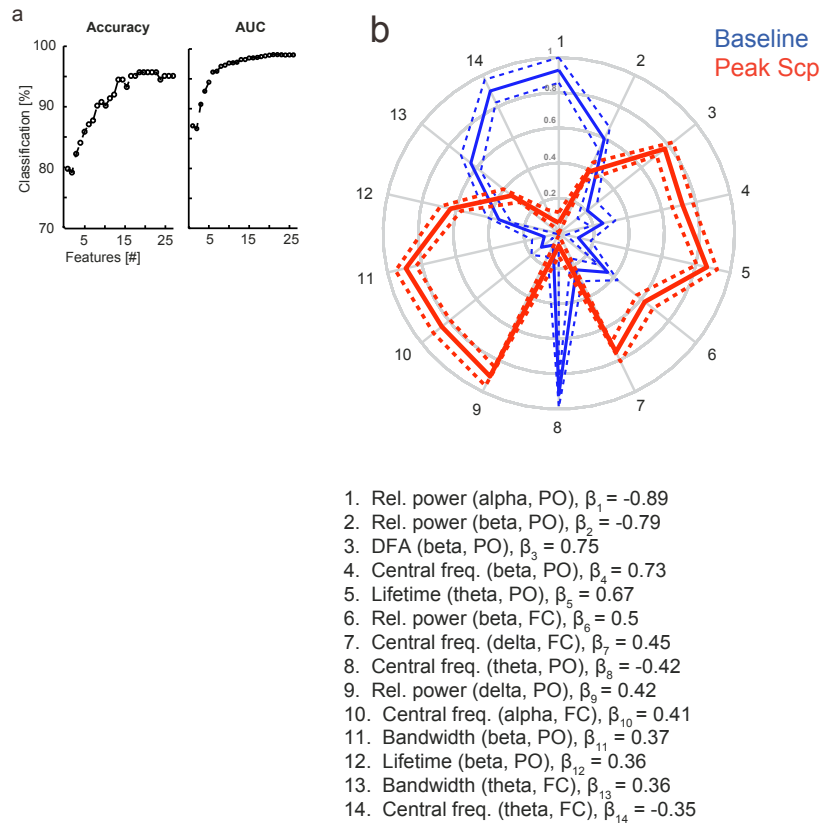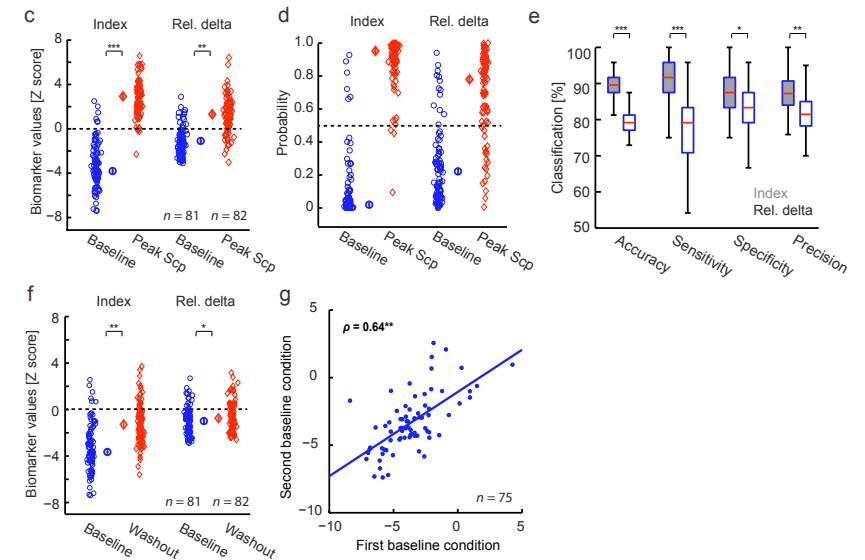
FIGURE 7.3-2

C. The mAChR index was more sensitive to the scopolamine (SCP) intervention than relative delta power. The plot shows z-scored biomarker values per subject recording. Singled-out symbols represent median values per group with standard error bars. The dashed line indicates the threshold of the classifier to predict the recordings as a baseline (below) or a peak scopolamine (above) recording. **D**. Same as C. but instead of z-scored biomarker values, predictive probabilities obtained from the classifier are shown. **E**. Classification performance of baseline vs scopolamine at the peak drug effect using 100 cross-validations is significantly higher for the mAChR index (**grey** boxplots) than the relative delta power (**white** boxplots). **F**. The superiority of the integrated index was also pronounced at washout. Relative delta power in the scopolamine condition was almost back to normal at 8.5 h after administration, whereas the mAChR index produced a highly significant effect. **G**. The integrated index has high test-retest reliability across weeks.

1. Rel. power (alpha, PO), β_1 = -0.89
2. Rel. power (beta, PO), β_2 = -0.79
3. DFA (beta, PO), β_3 = 0.75
4. Central freq. (beta, PO), β_4 = 0.73
5. Lifetime (theta, PO), β_5 = 0.67
6. Rel. power (beta, FC), β_6 = 0.5
7. Central freq. (delta, FC), β_7 = 0.45
8. Central freq. (theta, PO), β_8 = -0.42
9. Rel. power (delta, PO), β_9 = 0.42
10. Central freq. (alpha, FC), β_{10} = 0.41
11. Bandwidth (beta, PO), β_{11} = 0.37
12. Lifetime (beta, PO), β_{12} = 0.36
13. Bandwidth (theta, FC), β_{13} = 0.36
14. Central freq. (theta, FC), β_{14} = -0.35

Significance levels legend for this figure: * denotes $p < 0.05$, ** $p < 10^{-10}$, *** $p < 10^{-20}$, using Wilcoxon rank sum test.

FIGURE 7.4   The mAChR index generalizes to a new cohort of subjects.

A. The mAChR index also generalizes to a cohort of healthy elderly subjects receiving the same scopolamine intervention (Trial 3), with validation accuracy 87%, sensitivity 83%, specificity 91% and precision 91%. **B**. Time dependence curves demonstrate the generalizability of the index at all the time points. The mAChR index for placebo (**black**) and scopolamine (**red**) is shown for Trials 1 and 2 used for developing the index and for independent data from Trial 3 (in the latter there was no placebo condition). The values plotted are group means and standard errors of the mean computed for the within-subject design (Franz and Loftus, 2012).
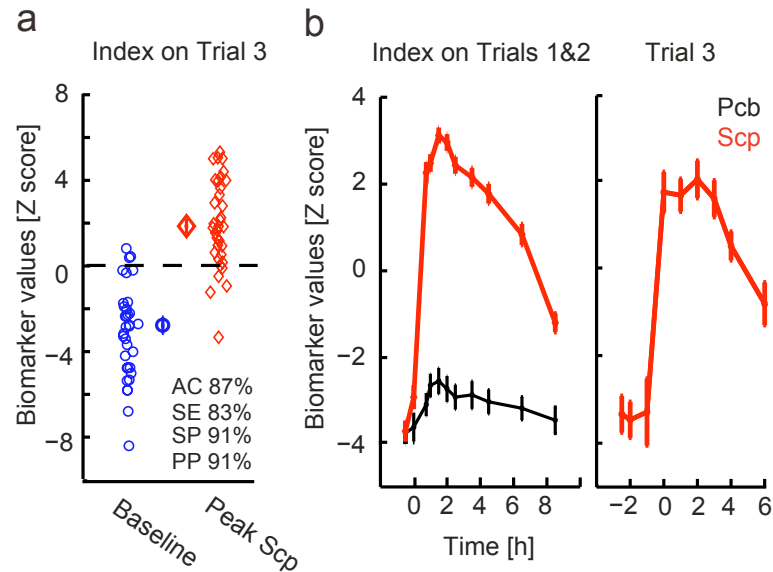
FIGURE 7.5-1   The integrated A D index captures scopolamine-induced effects and validates scopolamine as a model of A D pathophysiology.

A. Illustration of the twelve biomarkers composing the integrated Alzheimer's index. Several of these biomarkers also compose the scopolamine index, with the same directionality of change in both the scopolamine-induced cognitive impairment and Alzheimer's disease. The values plotted are as explained in Figure 7.3B. **B**. Integrated AD index separates healthy elderly from Alzheimer's disease patients with high precision. **C**. The mAChR index discriminates the healthy elderly and AD patients albeit less accurately than the AD index. **D**. Validating the AD index on the scopolamine data gives much better discrimination.
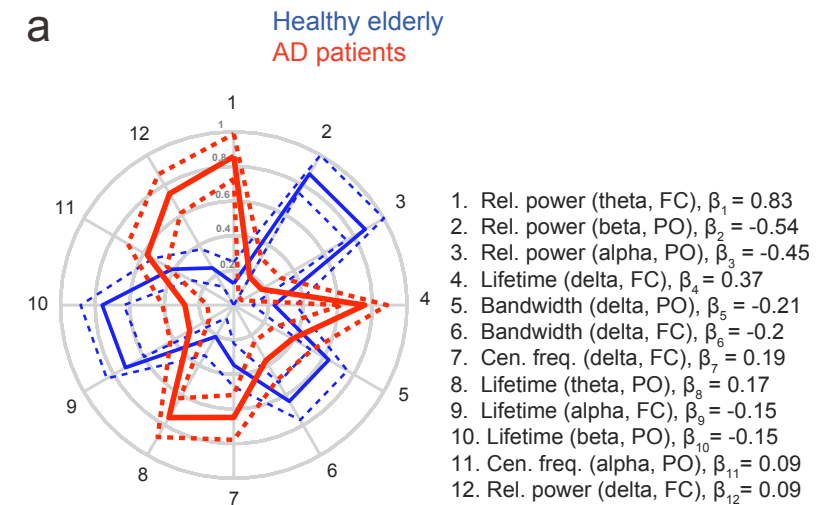
B. Integrated AD index separates healthy elderly from Alzheimer's disease patients with high precision. **C**. The mAChR index discriminates the healthy elderly and AD patients albeit less accurately than the AD index. **D**. Validating the AD index on the scopolamine data gives much better discrimination.